HIGH-ENERGY MILLING OF COMMERCIAL KAOLIN TO IMPROVE PLASTICITY FOR USE IN PORCELAIN TILES

Jorge Luiz Bombazaro [1,2], Angela Waterkemper Vieira [1,2], Sergio Ruzza [1], Adriano Michael Bernardin [2]

[1]Eliane Revestimentos Cerâmicos, Cocal do Sul, Santa Catarina, Brazil
[2]Graduate Program on Materials Science and Engineering, Universidade do Extremo Sul Catarinense, Criciúma, Santa Catarina, Brazil

ABSTRACT:

Plastic clays, or ball clays, are the most important clay minerals for ceramic tile production. They present high content of fine particles, high plasticity, low iron content, sedimentary origin, varied content of organic matter and kaolinite is the predominant clay mineral. They influence rheology, plasticity, green strength and are essential for compaction during pressing. In Brazil, there is a significant lack of deposits of plastic clays with adequate characteristics to produce porcelain tiles, but there are large reserves of kaolin. Therefore, this work aimed to physically change two kaolins used in a ceramic industry, yielding properties like those of plastic clays. Two commercial kaolins, one of low crystallinity and low purity (R) and the other of high crystallinity and high purity (I) were used. A commercial clay (M) was used as a plasticity standard. Initially, the kaolins were subjected to high-energy milling (Netzsch LabStar Discus attrition mill, 30 to 180 min of milling time) to physically alter the kaolinite. The high-energy milled kaolins were characterized by their plasticity index, particle size, and displacement of kaolinite peaks by X-ray diffraction. As a result, there was an increase in the plasticity and reactivity of R and I kaolins with the physical change caused by milling in a high-energy mill.

1. INTRODUCTION

Currently, Brazil is the 3rd largest producer and consumer market of ceramic tiles in the world, behind China and India. Brazilian tile production increased from 473 to 840 million m² from 2001 to 2020. In the same period, the Brazilian production of porcelain tiles increased from 4 to 168 million m² (Anfacer, 2021). As a result, the demand for suitable raw materials for producing porcelain tiles has increased.

In Brazil, the main deposits of plastic clays for ceramic tile processing are in the São Paulo and Piauí states (Laursen et al., 2019). There is a shortage of plastic clays in Santa Catarina state, where the production of porcelain tiles is prevalent.

On the other hand, there are large reserves of kaolin throughout Brazil. 95% of an estimated 15 billion tons of kaolin are in USA (53%), Brazil (28%), Ukraine (7%) and India (7%). The Brazilian reserves of kaolin account for 4.2 billion tons (USGS, 2021). Despite the large production of natural kaolin in Brazil, there is no production of modified kaolin for ceramic processing, although there is production of fine and calcined kaolin for rubber and plastics. Therefore, there is a need to process / modify natural kaolin for ceramic tile processing.

High-energy milling (HEM) is a processing technique used to change the environment of chemical reactions, improving the reactivity of solids by mechanical activation. HEM can increase reaction rates by reducing the reaction temperature of powders, or inducing chemical reactions during milling, which is called mechanochemistry (Ghayour et al., 2016; Compri et al., 2019; Mursalat et al., 2019; Leal et al., 2020; López-García et al., 2021). HEM can induce structural modifications of precursor powders by inducing their amorphization, polymorphic transformations, among other effects (Rianna et al., 2018; Shkodich et al., 2018; Rojas-Chávez et al., 2020; Sydorchuk et al., 2021).

Therefore, the aim of this work was to physically modify two kaolin used in commercial porcelain tile composition by high-energy milling to improve their plasticity during the pressing step.

2. MATERIALS AND METHODS

Two commercial kaolins, one of low crystallinity and low purity (R) and the other of high crystallinity and high purity (I) were used. A commercial clay (M) was used as a standard for the plasticity index. Both kaolins were ground in a laboratory ball mill for 30 min with 40 mass % of water (alumina balls and jar, 60/40: balls/kaolin by volume, φ = 10-15 mm) before characterization and high-energy milling. No deflocculant was used.

Before and after high-energy milling, the particle size distribution was determined by laser diffraction (CILAS 1064, 50 nm to 500 μm range).

Chemical analysis was determined by X-ray fluorescence (XRF) (Oxford Instruments X-Supreme). The structural change was determined by X-ray diffraction (XRD) (Shimadzu XRD 6100, Cu $_{K\alpha}$ (λ = 1.54 Å), 40 kV and 30 mA, 2θ 4 – 70°, 2°/min).

The Hinckley index (HI) was used to determine the degree of order/disorder of kaolinite based on the d110 and d111 reflections (2θ 20 to 23°). The d110 and d111 reflections are well defined for a highly ordered kaolinite. For high crystallinity or ordering IH > 1.0.

The plasticity index was determined by the indentation method. The load (N) to deform the kaolin paste in function of the moisture content (mass %) was determined. The plasticity index (PI) was calculated considering the difference in the consistency of the liquid limit (LL = 1 N), when the paste starts to flow, with regard to that of the plastic limit (PL = 46 N), when the paste is not deformable anymore, PI = LL – LP (Andrade et al., 2011).

The specific surface area and porosity of the kaolin samples were determined by the BET technique (Quantachrome Nova 1200e). The pH of both kaolins was determined in deionized water suspensions using a pHmeter (LEE W3B). Conductivity was performed using a conductivity meter (LEE W120). The cation exchange capacity (CEC) (mol/g) was analyzed by atomic absorption spectroscopy (Thermo Ice3000) for the presence of the Na, K, Ca and Mg elements in the samples.

A high-energy mill (Netzsch LabStar Discus, 2450 rpm, 60 °C) was used with zirconia beads (ZetaBeads, 3.65 kg/L, φ = 0.3-0.4 mm, 85 vol%). The water content was 65 wt%. No deflocculants were used.

The micronized kaolins were used in an industrial porcelain tile composition (Table 1) replacing the original kaolin R at 18.5% mass content. Initially, the porcelain tile composition was formed without any kaolin.

Raw material	Content (wt%)
Porcelain tile residue	6
Talc	2.5
Mixed clays	43.5
Nepheline	10.5
Feldspar	4
Granite	15
Kaolin R	18.5

***Table 1**. Industrial porcelain tile composition*

The composition was ground in an eccentric ball mill (alumina balls and jar, φ = 10 – 15 mm) for 10 min with 30% by mass of water. 60% of the mill volume was filled with the alumina balls. 0.5% of sodium silicate was used as dispersant. After milling, a control ceramic suspension was formed.

The control ceramic suspension (ceramic slip) was dispersed in 60 wt% water for homogenization and the micronized kaolin suspensions were added to the control suspension. Each kaolin suspension was added to the control suspension considering a content of 18.5% of each kaolin, on a dry basis.

The resulting porcelain tile slips with the micronized kaolin suspensions (micro-kaolin R and micro-kaolin I) were mixed and homogenized. The suspensions were dried for 12 h at 125 ± 5 °C. The dried powders were disaggregated in a hammer mill and mixed with 7% water. The moistened powder was passed through a 0.5 mm sieve for granulation. After granulation, the powders were pressed in an electro-hydraulic press (Nannetti Mignon) at 30 MPa in disk shapes with 40 mm diameter and 10 mm height. 10 specimens were pressed for each composition. The compacts were dried for 12 h at 125 ± 5 °C. After pressing and drying, the size, mass and apparent density of the samples were determined.

The samples were fired in a laboratory electrical roller kiln (Servitech CT350) for 30 min at five different temperatures ranging from 1,160 to 1,210 °C. The size, mass and water absorption of the samples were determined after firing.

The size of the samples after pressing and firing were determined using a caliper (0.1 mm resolution). The mass of the samples was determined using a scale (0.1 g resolution). The apparent density (d_{app}) of the samples was determined by measuring the volume (V) of the samples and their masses (m), where d_{app} = m/V (g/cm^3). The water absorption (WA) of the samples after firing was determined according to ISO 10545-3 (2018). The water absorption is a measure of the open porosity of the samples (%), and for porcelain tiles, according to ISO 10545-3 (2018), WA < 0.5%. Finally, the shrinkage (Sh) of the samples was also determined after firing. The shrinkage is used to determine the degree of densification of a tile composition during firing. Sh is the difference of the size of the samples after firing, considering the size before firing, Sh = $(d_f - d_0)/d_0$, where d_f is the final size of the sample, and d_0 is the initial size.

The performance of the micronized kaolins was measured by determining their vitrification curve. Vitrification curves are graphs where the firing shrinkage and water absorption of a specific tile composition are evaluated at different temperatures. They are used to determine if the tile compositions meet the water absorption requirements for their class (in this case, porcelain tiles, which must show WA < 0.5%) under the processing conditions (mainly firing cycles). They can also show the dimensional stability of the composition as a function of size changes (firing shrinkage) with temperature.

3. RESULTS AND DISCUSSION

Particle size can change clay plasticity. Thinner clays are plastic in water. Plastic clays generally show 80 wt% of their particle sizes below 2 μm (Almeida et al., 2021). Bentonites show particle sizes ranging from 2 – 0.1 μm, with an average size of ~0.5 μm (Andrade et al., 2011). High-energy milling was used in this work to reduce the kaolin particles to submicron sizes. Traditional milling methods cannot reduce kaolin particle size below μm.

The particle size distributions (PSD) – cumulative and density distributions – before and after the high-energy milling for both kaolins are shown in Fig.2. After HEM, a narrowing of the particle size distribution is noticed at 1 μm for kaolin I (Fig.1(a)). Before milling the distribution was centered at 6.5 μm. The HEM process was more effective for kaolin R (Fig.1(b)): the particle size distribution was centered at 10 μm before milling, after milling, the distribution became centered at 800 nm.

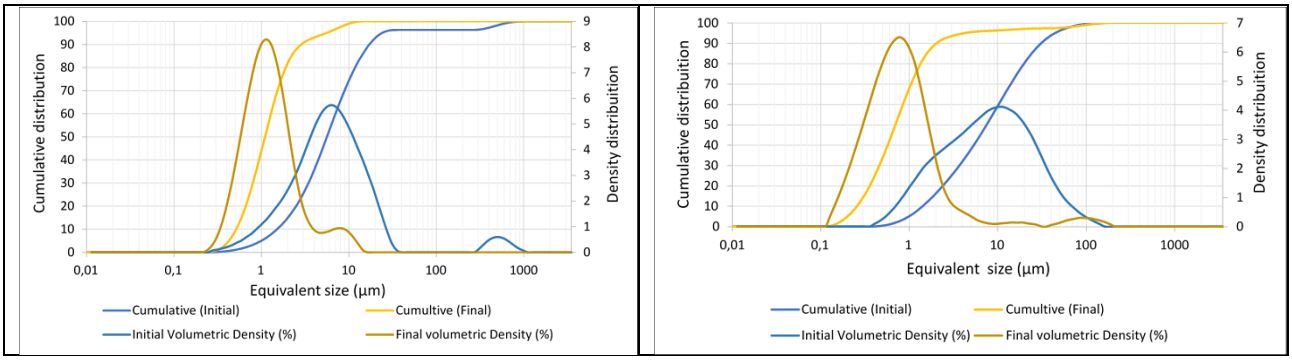

Figure 1. *Particle size distribution before (initial) and after (final) high-energy milling for kaolin I (a) and R (b)*

After HEM, 84% of the PSD of kaolin I and 91% PSD of kaolin R was < 2 μm. 11% of the particle size distribution of kaolin I and 36% of kaolin R was < 0.5 μm. Therefore, HEM was fully effective for kaolin R (D_{50} = 700 nm after 120 min milling) and partially effective for kaolin I (D_{50} = 1.1 μm after 180 min milling).

Kaolin I is formed only by kaolinite (JCPDS 29-1488), a soft mineral with low hardness (Fig.2) that is more difficult to mill just because of its plastic behavior. Kaolin R is formed by kaolinite (JCPDS 29-1488), anorthosite (JCPDS 20-0528), and quartz (JCPDS 46-1045) (Fig.5). Quartz and anorthosite are harder materials; therefore, kaolin R was easier to mill into smaller particle sizes.

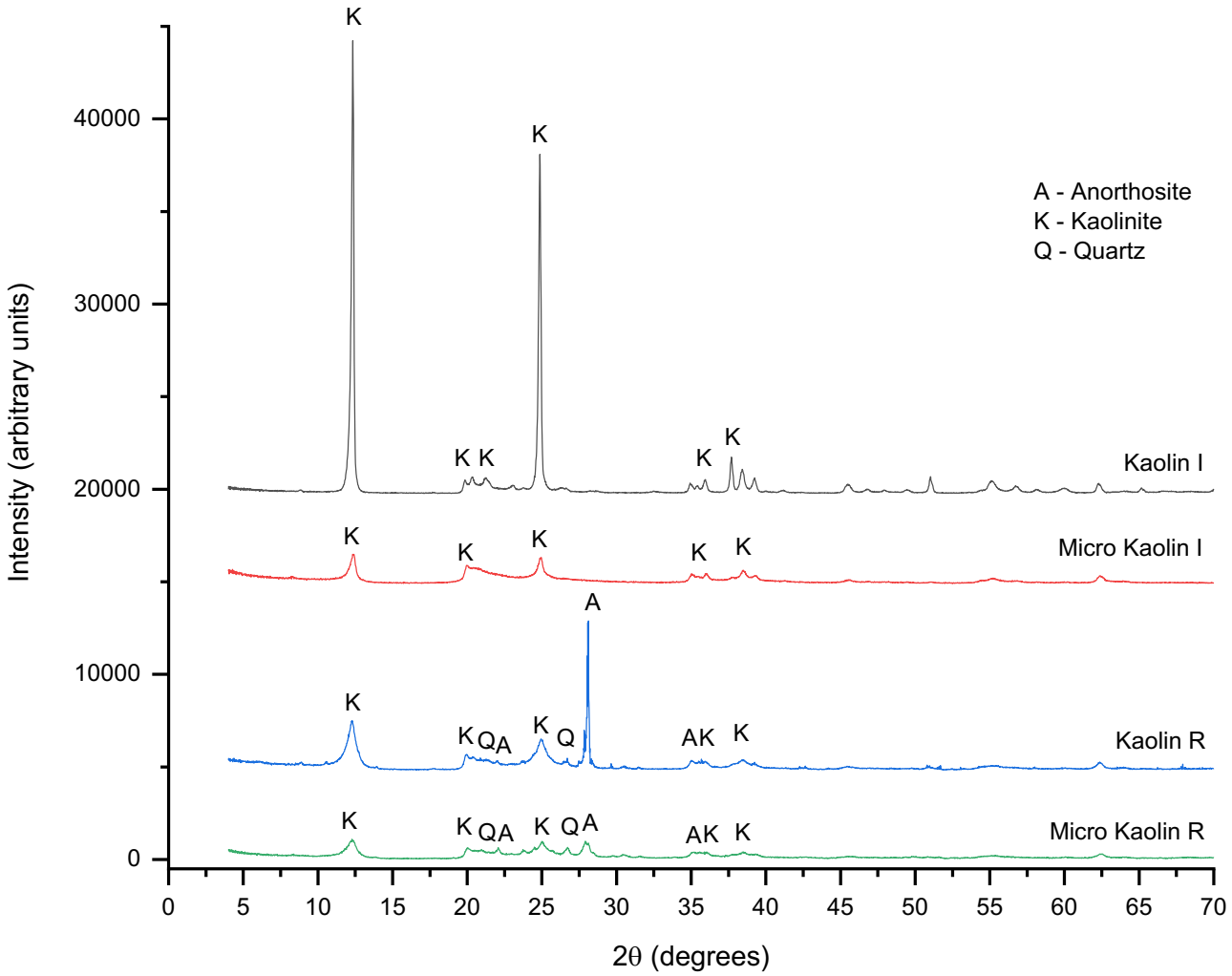

***Figure 2**. X-ray diffraction of kaolin I and kaolin R before and after high-energy milling*

After milling, the crystallinity (structural ordering) of both kaolins had decreased due to the changes in the peaks height at 20 – 25° (2θ). The disordering could increase the plasticity of both kaolins. For kaolin R, the peak at 26° (2θ) referenced quartz shows that the reduction in particle size also reduces the intensity of the peaks after milling (Fig.2). Before milling, the Hinckley indices were HI = 1.00 for kaolin I, a high crystallinity index, and HI = 0.37 for kaolin R, low crystallinity. After milling both kaolins showed low crystallinity as HI < 0.3. Therefore, the HEM process was very effective in changing the ordering of the crystalline structure of both materials, mainly for kaolin I (Fig.2).

The reduction in particle size has increased the plasticity of the samples, as given by the plasticity index (PI) (Fig.3). There was an increase in PI of both kaolins after high-energy milling. Therefore, HEM increased the plasticity of both kaolins (Fig.3), that is, small particle sizes are characteristic of plastic materials. Kaolin R PI increased by 95%, from 13.0 to 25.3 after milling. The PI of kaolin I changed from 10.0 to 26.3, an increase of 163%. Micro-kaolin I, with larger particle size, showed higher plasticity than micro-kaolin R. Kaolin R is not a pure clay mineral and shows quartz and anorthosite in its composition (Fig.2), not presenting plasticity in water.

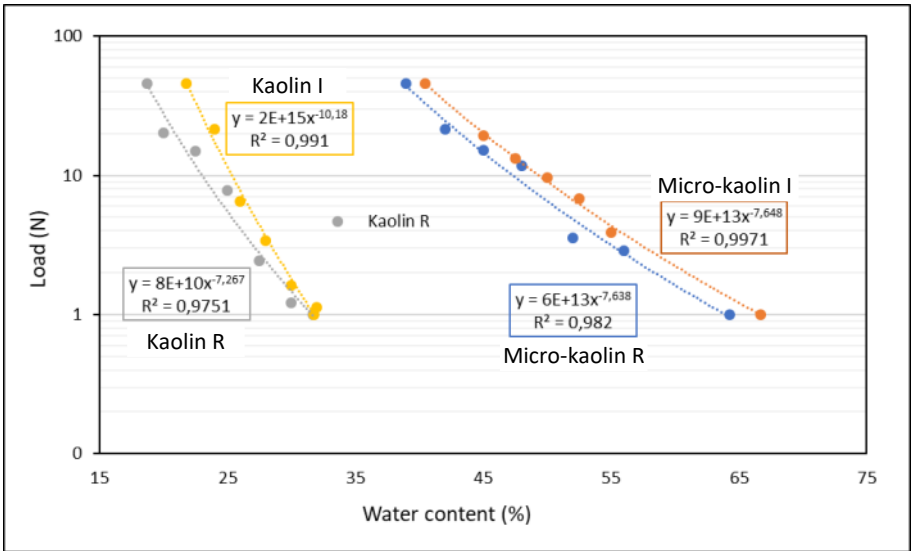

***Figure 3**. Plasticity index (PI) of kaolins R and I before and after high-energy milling*

The surface area and pore volume of the samples before and after high-energy milling are shown in Table 2. There was a large increase in the specific surface area (SSA) and pore volume after milling for both kaolins. The SSA of micro-kaolin I was greatly increased from 5.5. to 186 m^2/g. As the particle size after HEM was smaller for kaolin R than for kaolin I, probably the large increase in SSA for the latter is due to more defects and pores induced by HEM, because the pore volume for kaolin I after milling was increased by 2400%.

	Kaolin R	Micro-kaolin R	Kaolin I	Micro-kaolin I
Specific surface area (m^2/g)	17.2	47.3	5.5	186.4
Total pore volume (cm^3/g)	4.8×10^{-2}	21×10^{-2}	1.9×10^{-2}	49×10^{-2}

***Table 2**. Specific surface area (m^2/g) and pore volume (cm^3/g) of kaolins R and I before and after high-energy milling*

The pH and conductivity of both samples are shown in Table 3. Kaolin R had a large increase in conductivity (536%) and pH (56%) after milling. Probably, the HEM process has destroyed the structure of the minerals (kaolinite and anorthosite) and released some ions into the solution, as Ca^{2+}, Mg^{2+}, and Na^{+} (Table 4).

The conductivity of kaolin I (and micro-kaolin I) is higher (Table 3) because this mineral undergoes a purification process with the use of deflocculants, increasing the amount of Na^{+} ions in the suspension after milling (Table 4).

	Deionized water	Kaolin I	Micro-kaolin I	Kaolin R	Micro-kaolin R
pH	6.23	5.06	6.56	5.92	9.21
Conductivity (µS/cm)	2.64	162.20	252.67	21.63	140.4

Table 3. *pH and conductivity of kaolins R and I before and after high-energy milling*

The cation exchange capacity (CEC) of the samples before and after high-energy milling is shown in Table 4. There was an increase in the cation exchange capacity for both kaolins, smaller for kaolin R (86%), higher for kaolin I (488%). The change in CEC may be due to the release of Na^{+}, Mg^{2+}, and Ca^{2+} ions during milling.

Ion	Kaolin I	Micro-kaolin I	Kaolin R	Micro-kaolin R
Na^{+}	1.93	9.81	1.09	3.68
K^{+}	0.56	2.1	0.37	0.69
Mg^{2+}	0.46	1.61	0.75	2.48
Ca^{2+}	1.06	10.02	1.67	7.87
Total	4.02	23.54	6.47	12.14

Table 4*. Cation exchange capacity (CEC) of kaolins R and I before and after high-energy milling*

3.2. USE OF HIGH-ENERGY MILLED KAOLIN ON PORCELAIN TILE COMPOSITION

The apparent density of the samples was used to evaluate the effect of high-energy milling of both kaolins during pressing (Table 5). The composition with kaolin R was used as a standard. There was a reduction in the apparent density of the pressed samples when the high-energy milled kaolins were used in the compositions. Low density porcelain tiles are not appropriate for ceramic processing because they exhibit high porosity after firing.

Compositions	Moisture (%)	SD	Apparent density (g/cm³)	SD
Kaolin I	7.75	0.13	1.92	0.010
Kaolin R	7.84	0.05	1.97	0.001
Micro-kaolin I	7.23	0.12	1.85	0.001
Micro-kaolin R	7.15	0.05	1.88	0.001

Table 5. *Apparent density of the porcelain compositions after pressing using kaolins R and I before and after high-energy milling*

The increase in the specific surface areas of the compositions using the high-energy milled kaolins has increased the number of contacts among the particles and, consequently, their friction.

The shape of the particles also changes the densification. Micro-kaolin I showed the highest plasticity index and the lowest density when used in the porcelain tile composition. Besides not showing the finest particle size distribution, micro-kaolin I is almost entirely formed by lamellar particles with higher aspect ratio (kaolinite). On the other hand, micro-kaolin R is formed by minerals with lower aspect ratio of irregular to spherical shapes (quartz and anorthosite), with better densification.

The densification of the porcelain tile compositions may be related to other factors such as the specific surface area of the particles and the electrostatic interactions between particles. The increase in the specific surface area of the kaolins after high-energy milling apparently has increased the friction between the particles during compaction, impairing the densification, even with the increased plasticity of the materials.

Considering the electrical charges and interactions between particles that promote plasticity, an analysis was made of the probable causes of the unexpected behavior of reducing the density of the porcelain tile compositions when using more plastic materials. Probably there was a correlation between rheological properties (flow stress) and plasticity.

The difference in the analysis and characterization of the raw kaolins and when they were used in the tile compositions was the use of deflocculants/dispersants in the latter. The plasticity measurements are carried out in the natural condition of the raw materials, without the use of additives, as well as the rheological analysis. However, dispersing/deflocculating agents are used in the production of ceramic tile compositions to enable the milling and spray-drying processes. Analyzing the action mechanism of dispersants/deflocculants, to disperse the particles, the deflocculant must eliminate the interactions between them, therefore, directly interfering with the plasticity of the materials. Hypothetically, the deflocculation mechanisms should reduce the plasticity of the materials, as they reduce the viscosity of suspensions containing clay minerals (rheology × plasticity ratio).

To prove this hypothesis, tests were carried out with clay M, one of the raw materials of the porcelain tile composition and the most plastic clay. The plasticity index of clay M in natura and after being deflocculated with 2.0% (in mass) of sodium silicate was determined by the indentation method.

For comparison, the plasticity index for clay M before and after deflocculation is shown in Fig.4. In natura, clay M shows high plasticity. After deflocculation, the plasticity index of clay M was reduced to less than 50%, showing that the use of deflocculants during the milling process of ceramic tile compositions can reduce their plasticity during pressing.

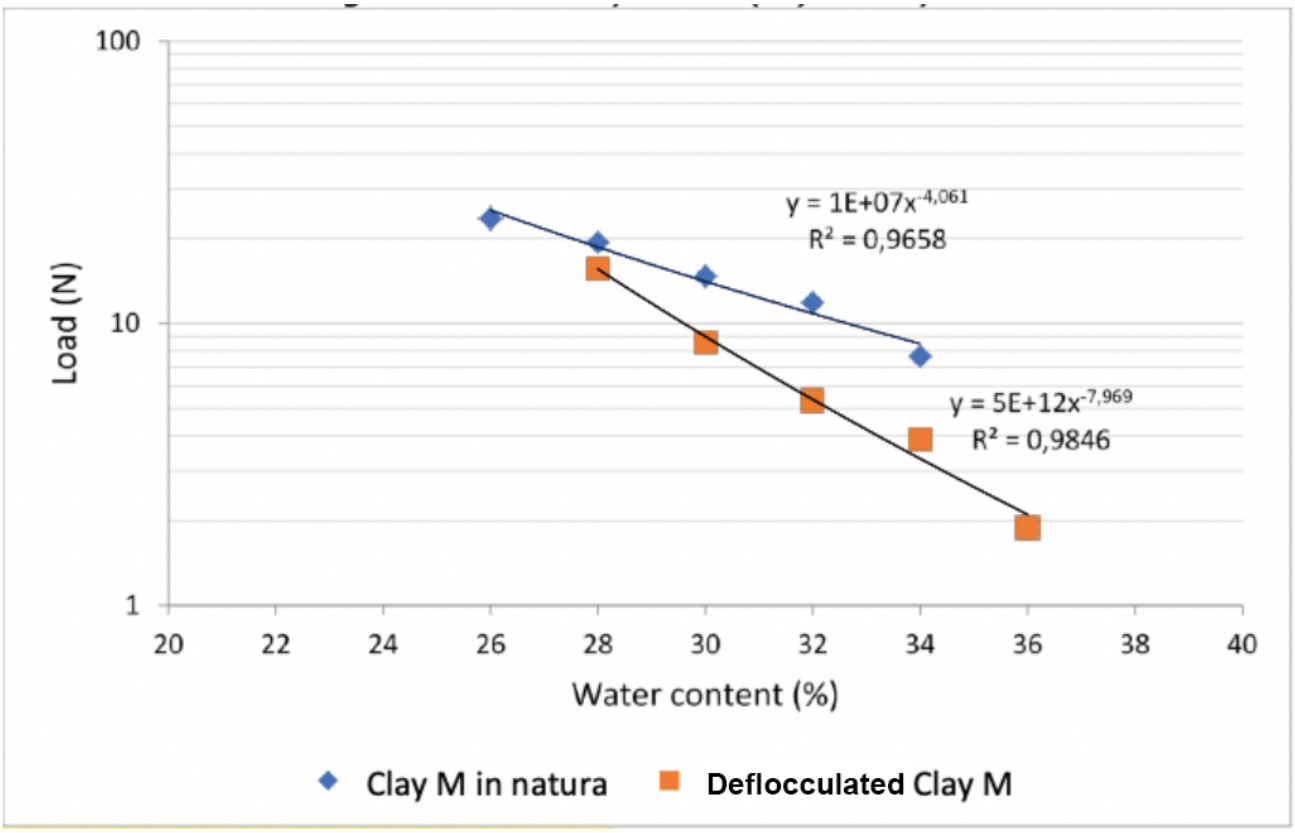

***Figure 4**. Plasticity index (PI) of clay M before and after deflocculation*

3.3. EFFECT OF HIGH-ENERGY MILLING ON THE FIRING CHARACTERISTICS OF A PORCELAIN TILE COMPOSITION

To evaluate the sintering behavior of the porcelain tile compositions using kaolins R and I before and after the high-energy milling, gresification diagrams were studied for the shrinkage and water absorption of the compositions in function of temperature (Fig.5). For all compositions, the kaolin content (before and after high-energy milling) was 18.5% (by mass).

The shrinkage of the composition with kaolin R was 7.2 – 7.3% in the temperature range of 1160 – 1200 °C. Water absorption ranged from 0.1% to 0.5%. The presence of anorthosite in kaolin R, a mineral rich in calcium, made this composition more reactive during firing. The composition with micro-kaolin R showed a shrinkage ranging from 8.1 – 9.3% and water absorption ranging from 0.0 – 0.1% for the temperature range of 1160 – 1200 °C. Therefore, high-energy milling increased the reactivity of the composition due to the lower water absorption. The greater shrinkage is due to the lower apparent density after compaction (see Table 4).

For the porcelain tile composition using kaolin I (Fig.5), the shrinkage changes from 8.2% to 8.5% and the water absorption from 0.2% to 1.2% in the temperature range of 1170 – 1210 °C. Kaolin I is a refractory material due to the presence of kaolinite, as evidenced by the higher water absorption of the composition. The shrinkage of the composition with micro-kaolin I was 9.1 – 9.3% for the temperature range of 1170 – 1210 °C, with a water absorption of 0.1 – 0.7% for the same temperature range. There was a considerable increase in reactivity with the high-energy milled kaolin. The higher shrinkage is due to the lower apparent density after compaction in comparison with the composition using kaolin I.

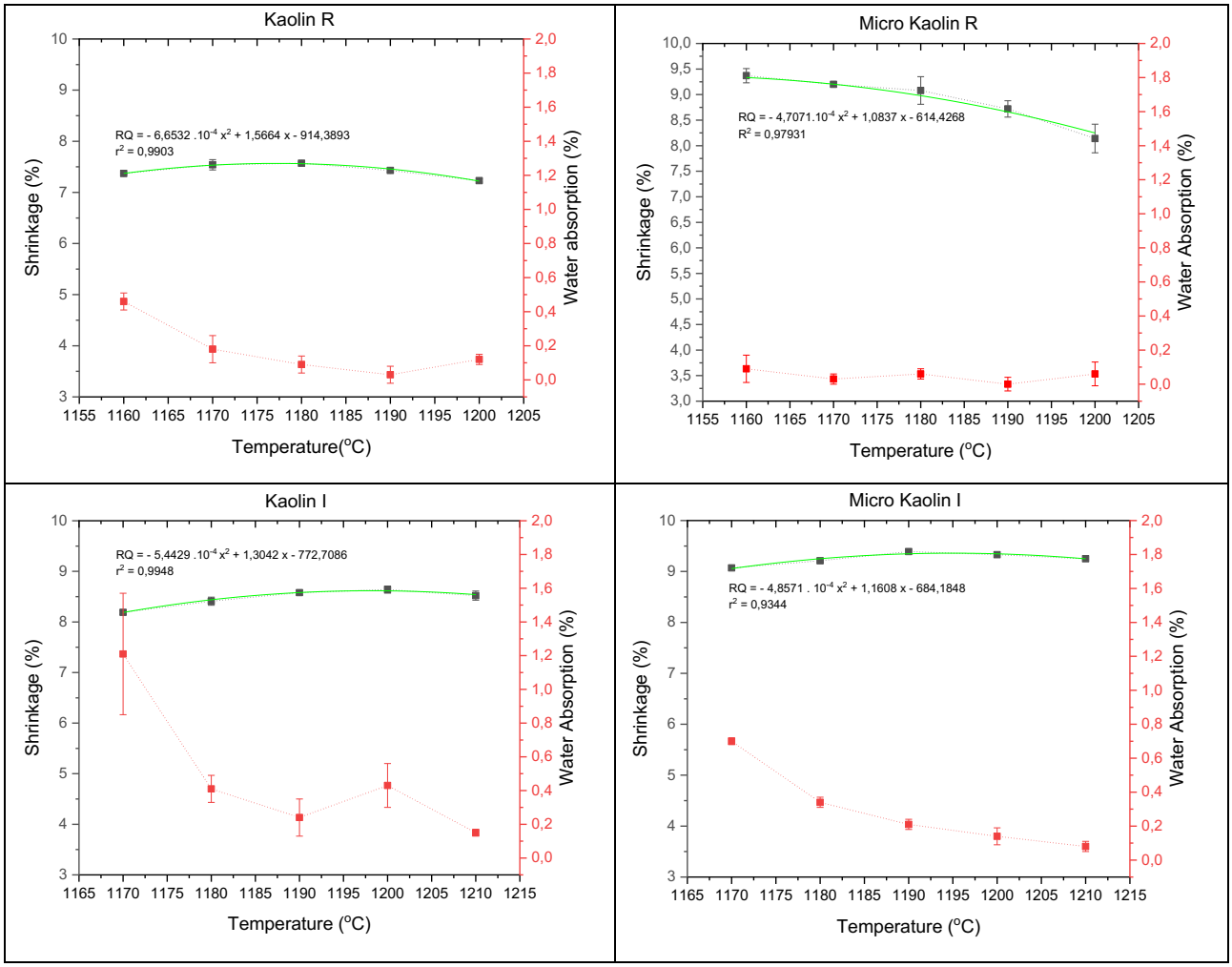

***Figure 5**. Gresification diagrams (shrinkage and water absorption × temperature) for the porcelain tile composition using kaolins R and I before and after high-energy milling*

The high-energy milled kaolins gave rise to compositions with lower sintering temperatures, given by the reduction of water absorption due to the increased reactivity that the micro-kaolins provided to the porcelain tile composition. Kaolin R contains fluxing oxides that help sintering, given by the content of alkali and alkaline earth metal oxides in its composition, mainly Na_2O, K_2O, MgO and CaO (Table 6). Therefore, the increase in sinterability of the porcelain tile compositions is related to the reduction in particle size due to the high-energy milling of kaolins R and I and due to the presence of fluxing oxides, specifically in kaolin R.

The compositions with kaolin I and micro-kaolin I only show water absorption below 0.5% (water absorption limit for porcelain tiles) at temperatures above 1180 °C due to the refractoriness of kaolin I that is formed mainly by kaolinite. The composition with micro-kaolin I shows an increased reactivity at 1170 °C. At this temperature, the water absorption of the composition decreased from 1.21% with kaolin I to 0.70% with micro-kaolin I.

Oxide	Kaolin I	Kaolin R
Al_2O_3	42.6	35.6
CaO	0.0	2.6
Fe_2O_3	0.4	1.4
K_2O	0.0	0.5
MgO	0.4	0.8
Na_2O	0.4	0.9
SiO_2	41.3	44.4
SO_3	0.6	0.2
TiO_2	0.4	0.2
LoI	19.2	11.4

***Table 6**. Chemical analysis of kaolins R and I by X-ray fluorescence*

CONCLUSIONS

Two commercially available kaolins used in porcelain tile compositions were processed in this work by high-energy milling to improve their plasticity during the forming process.

After high-energy milling, 84 – 91% of the particle size distribution of both kaolins was < 2 μm, showing the effectiveness of the HEM process to reduce the particle size of the materials.

There was a reduction in the crystallinity (ordering) for both kaolins, resulting in microstructures that could increase the plasticity of both materials.

High-energy milling increased the plasticity of both kaolins by 95 – 163 %, showing that small particle sizes are characteristic of plastic materials.

The specific surface areas (SSAs) were increased by 176 – 3,000 % after HEM. But the cation exchange capacity (CEC) was increased by 50% for kaolin R and by 488% for kaolin I, showing that the original characteristics of the raw materials change their processability by high-energy milling. Kaolin I is a pure mineral, but kaolin R was contaminated with quartz and anorthosite.

When both high-energy-milled kaolins were used in a porcelain tile composition (18.5 mass % addition), there was a reduction in the apparent density of the pressed samples besides the higher plasticity of the milled kaolins. The increase in the specific surface area of the kaolins after high-energy milling apparently has increased the friction between the particles during compaction, impairing densification, even with the increased plasticity of the materials.

After HEM, the shrinkage of the porcelain tile compositions changed from 7.2 – 8.5% to 8.1 – 9.3% and water absorption changed from 0.1 – 1.0% to 0.0 – 0.7% in the temperature range of 1160 – 1210 °C. Therefore, high-energy milling can increase the reactivity of refractory materials such as kaolins.

Despite the higher firing shrinkage, the compositions achieved better dimensional stability. For industrial uses, it is necessary to determine the best relationship between particle size reduction and energy cost. The results show that the right choice of raw material to be processed by high-energy milling and the degree of particle size reduction can be the key to making high-energy milling applicable in industrial production.

REFERENCES:

[1] Almeida E P, Carreiro M E A, Rodrigues A M, Ferreira H S, Santana L N L, Menezes R R, Neves G A, 2021. A new eco-friendly mass formulation based on industrial mining residues for the manufacture of ceramic tiles. Ceramics International 47, 8, 11340-11348. https://doi.org/10.1016/j.ceramint.2020.12.260

[2] Andrade F A, Al-Qureshi H A, Hotza D, 2011. Measuring the plasticity of clays: A review. Applied Clay Science 51, 1–2, 1-7. https://doi.org/10.1016/j.clay.2010.10.028

[3] ANFACER, 2021. Ceramics Sector Numbers. Brazilian Association of Manufacturers of Ceramics for Coatings, Sanitaryware and Like Products. https://www.anfacer.org.br/setor-ceramico/

[4] Compri J C Z, Felli V M A, Lourenço F R, Takatsuka T, Fotaki N, Löbenberg R, Bou-Chacra N A, Araujo G L B, 2019. Highly water-soluble orotic acid nanocrystals produced by high-energy milling. Journal of Pharmaceutical Sciences 108, 5, 1848-1856. http://dx.doi.org/10.1016/j.xphs.2018.12.015

[5] Ghayour H, Abdellahi M, Bahmanpour M, 2016. Optimization of the high energy ball-milling: modeling and parametric study. Powder Technology 291, 7-13. http://dx.doi.org/10.1016/j.powtec.2015.12.004

[6] ISO 10545-1, 2014. Ceramic tiles. Part 1: Sampling and basis for acceptance. Geneva, Switzerland: International Organization for Standardization.

[7] ISO 10545-3, 2018. Ceramic tiles. Part 3: Determination of water absorption, apparent porosity, apparent relative density and bulk density. Geneva, Switzerland: International Organization for Standardization.

[8] Laursen A, Santana L N L, Menezes R R, 2019. Characterization of Brazilian Northeastern plastic clays. Cerâmica 65, 578-584. https://doi.org/10.1590/0366-69132019653762579

[9] Leal E A D, Gomes U U, Alves S M, Costa F A, 2020. The influence of powder preparation condition on densification and microstructural properties of WC-Co- Al2O3 cermets. International Journal of Refractory Metals and Hard Materials 92, 105275. http://dx.doi.org/10.1016/j.ijrmhm.2020.105275

[10] López-García J, Sánchez-Alarcos V, Recarte V, Rodríguez-Velamazán J.A, Unzueta I, García J.A, Plazaola F, Laroca P, Pérez-Landazábal J.I, 2021. Effect of high-energy ball-milling on the magnetostructural properties of a Ni45Co5Mn35Sn15 alloy. Journal of Alloys and Compounds 858, 158350. http://dx.doi.org/10.1016/j.jallcom.2020.158350

[11] Mursalat M, Schoenitz M, Dreizin E L, 2019. Composite Al·Ti powders prepared by high-energy milling with different process controls agents. Advanced Powder Technology 30, 7, 1319-1328. http://dx.doi.org/10.1016/j.apt.2019.04.007

[12] Rianna M, Sembiring T, Situmorang M, Kurniawan C, Setiadi E A, Tetuko A P, Simbolon S, Ginting M, Sebayang P, 2018. Characterization of natural iron sand from Kata Beach, West Sumatra with high energy milling (HEM). Jurnal Natural 18, 2, 97-100. http://dx.doi.org/10.24815/jn.v18i2.11163

[13] Rojas-Chávez H, Juárez-García J M, Herrera-Rivera R, Flores-Rojas E, González-Domínguez J L, Cruz-Orea A, Cayetano-Castro N, Ávila-García A, Mondragón-Sánchez M L, 2020. The high-energy milling process as a synergistic approach to minimize the thermal conductivity of PbTe nanostructures. Journal of Alloys and Compounds 820, 153167. http://dx.doi.org/10.1016/j.jallcom.2019.153167

[14] Shkodich N F, Vadchenko S G, Nepapushev A A, Kovalev D Y, Kovalev I D, Ruvimov S, Rogachev A S, Mukasyan A S, 2018. Crystallization of amorphous Cu50Ti50 alloy prepared by high-energy ball milling. Journal of Alloys and Compounds 741, 575-579. http://dx.doi.org/10.1016/j.jallcom.2018.01.062

[15] Sydorchuk V, Vasylechko V, Khyzhun O, Gryshchouk G, Khalameida S, Vasylechko L, 2021. Effect of high-energy milling on the structure, some physicochemical and photocatalytic properties of clinoptilolite. Applied Catalysis A: General 610, 117930. http://dx.doi.org/10.1016/j.apcata.2020.117930

[16] USGS, 2021. Clays. Mineral Commodity Summaries. United States Geological Survey. https://pubs.usgs.gov/periodicals/mcs2021/mcs2021-clays.pdf